

# The ISO spectrum of the planetary nebula NGC 6302

## I. Observations

D.A. Beintema<sup>1</sup> and S.R. Pottasch<sup>2</sup>

<sup>1</sup> SRON Laboratory for Space Research, P.O. Box 800, 9700 AV Groningen, the Netherlands

<sup>2</sup> Kapteyn Astronomical Institute, P.O. Box 800, 9700 AV Groningen, The Netherlands

Received 2 February 1999 / Accepted 9 April 1999

**Abstract.** The spectrum of the planetary nebula NGC 6302 is presented, as it was observed by the ISO short-wavelength spectrometer. The IUE spectrum observed at the same position with the same aperture is also presented.

**Key words:** stars: abundances – stars: evolution – ISM: planetary nebulae: individual: NGC 6302 – infrared: ISM: lines and bands

### 1. Introduction

The planetary nebula NGC 6302 has been known for a long time. It is rather difficult to describe because its optical image and its radio image differ enormously. This is mainly because there is a great deal of extinction. This extinction occurs very close to, or within, the nebula. A dark dust lane running approximately north south makes the central part of the nebula invisible in optical light. It also completely extinguishes the light from the central star, which consequently has never been seen. There is evidence (Ashley & Hyland, 1988; Pottasch et al. 1996) that the central star is the hottest object known in the galaxy.

The nebula is interesting from another point of view. The nitrogen abundance is very high, similar to the oxygen abundance. The conversion of so much oxygen to nitrogen in the course of the evolution of the star indicates that it was originally very massive, and the present remnant is also likely to be massive. There may be other abundance anomalies which can provide a clue to the nuclear processes which have occurred.

The extinction causes great difficulties in studying the nebular abundances. First of all, it is not known precisely where the material causing the extinction is located, although it is clear that it must be close to the nebula. But correcting an optical (or ultraviolet) spectrum assuming a constant average extinction (as is invariably done) is at best an approximation.

The use of an ISO spectrum improves this situation considerably: extinction effects are absent from most of the spectrum. In the short wavelength region some extinction correction is required, but it is only about 10% of the measured flux.

There are two other effects which can be substantially improved by using the ISO spectrum. First of all, only a limited number of ions of a given element are available in the optical spectrum; sometimes only a single ion. Often this ion is not the principal stage of ionization, so that a correction for the unseen ionization stages must be made. The theoretical basis for this correction is often uncertain, which makes the result “suspect”. The use of ISO spectra alleviate these problems to an important extent because so many ionization stages are observed in the infrared that no “guesses” as to the stellar ionizing radiation need to be made. Even stronger, the problem may be inverted and the stellar radiation field derived from the abundances of the various ionization states.

The other uncertainty in the interpretation of the optical and ultraviolet spectrum is due to the possibility of electron temperature inhomogeneities in the nebula. The lines in this spectral range have sufficient energies that their collisional excitation is strongly dependent on the temperature of the electrons. If the temperature is constant in the nebula, its value as determined by the observed O III line ratio’s may be used for all ions. If, however, it is inhomogeneous, it will affect lines of different energies in different ways, and using the O III temperature will lead to faulty results. This problem does not exist for the lines in the ISO infrared since their energies are small enough that the temperature dependence of the collisional excitation is quite small.

In this paper the observations made by the ISO short wavelength spectrograph (SWS) are presented. This will be supplemented by a presentation of the IUE spectrum which was taken at essentially the same position and with the same aperture as the SWS spectrum. It is our intention to analyse the total spectrum of this PN in the next paper in this series.

### 2. ISO observations

The ISO SWS observations were made with the SWS06 observing template, which provided complete spectral coverage at the full spectral resolution (1000 to 2000) of the SWS. The observations were made in February and March 1997. One observation provided coverage from 2.4 to 7  $\mu\text{m}$  and from 12 to 27.5  $\mu\text{m}$ , the second observation covered the spectrum from 7 to 12  $\mu\text{m}$  and from 28 to 45  $\mu\text{m}$ .

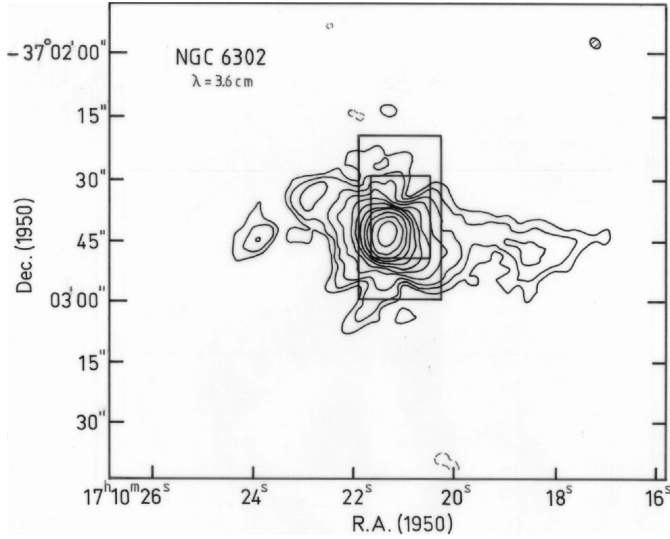


**Fig. 1.** The contours show the 3.6-cm radio continuum map of NGC 6302, made with the VLA. The beam is shown in the upper right. The highest contour is 307 mJy/beam. The contour levels change by a factor 2, so that the 3rd from the centre is the 12% level and the 6th is below the 3% level. Two SWS apertures are shown; the smaller aperture is for all wavelengths below  $12 \mu\text{m}$ , and the large aperture is for wavelengths above  $29 \mu\text{m}$ . There are intermediate apertures for intermediate wavelengths.

### 3. Position of aperture

The aperture was centred at the same position for both observations, to within 3 arc sec. In Fig. 1 the ISO aperture is superimposed on the 3.6 cm VLA radio continuum map of NGC 6302. The centre of ISO aperture is about  $5''$  NW of the radio center. The smallest aperture shown was used for measurements below  $12 \mu\text{m}$ , while the large aperture applies to SWS measurements above  $29 \mu\text{m}$ . For intermediate wavelengths, intermediate apertures were used. The position of the aperture center is uncertain by about  $3''$ .

The radio contours are successively a factor of two lower compared to the previous contour. This means that the 12% level is already reached by the 3rd contour from the centre. Thus while some of the flux is being missed, we expect at least 50%, and possibly more than 80%, is being measured by ISO. This could depend on the line measured.

The compactness of the source is confirmed by the observed dust continuum. We do not observe positive discontinuities in the spectrum where the aperture increases at  $27.5 \mu\text{m}$  and at  $29 \mu\text{m}$ . In fact, the spectrum between  $27.5$  and  $45.2 \mu\text{m}$  appears to be too low by about 20%, suggesting a misalignment.

In order to correct for the slight differences in pointing, and to correct for the differences in aperture size for the different wavelength regions, we have made use of the fact that there is a small overlap for the various wavelength bands. The intensities of the different spectra were adjusted to the smallest aperture,  $14'' \times 20''$ , so that the dust continuum was continuous. This required that the intensities of the lines between  $27.5$  and  $45 \mu\text{m}$

**Table 1.** Measured line intensities  $I$  in units of  $10^{-12} \text{ erg cm}^{-2} \text{ s}^{-1}$ , wavelength  $\lambda$  in  $\mu\text{m}$ . Mg VII is blended with Ar III.

$\lambda$	$I$	Ident.	$\lambda$	$I$	Ident.
2.406	1.19	H <sub>2</sub>	6.15	<0.2	Ca VIII
2.423	0.60	H <sub>2</sub>	6.491	2.82	Si VII
2.455	0.63	H <sub>2</sub>	6.702	2.39	Cl V
2.483	22.7	Si VII	6.906	1.86	H <sub>2</sub>
2.563	0.33	HI 15-5	6.945	1.40	He II 9-8
2.584	<0.1	Si IX	6.981	51.0	Ar II
2.624	5.9	HI 6-4 Br $\beta$	7.314	5.92	Na III
2.673	0.29	HI 13-5	7.458	4.13	HI 6-5 Pf $\alpha$
2.757	0.43	HI 12-5	7.499	1.14	HI 8-6
2.801	0.10	H <sub>2</sub>	7.648	627	Ne VI
2.825	1.22	HeII 9-7	7.813	<0.3	Fe VII
2.871	0.55	HI 11-5	7.898	21.5	Ar V
2.905	<0.02	Al V	8.021	0.70	H <sub>2</sub>
2.972	0.15	H <sub>2</sub>	8.607	10.7	Na VI
			8.757	0.25	HI 10-7
3.003	0.19	H <sub>2</sub>	8.826	0.44	K VI
3.027	2.0	Mg VIII	8.988	50.5	Ar III
3.038	0.66	HI 10-5	9.038	1.86	Na IV
3.091	3.25	He II 7-6	9.109	<0.14	Al VI
3.144	0.10	He II 14-9	9.523	0.50	Fe VII
3.189	0.46	K VII	9.661	1.74	H <sub>2</sub>
3.205	0.19	Ca IV	10.052	1.84	Cl II
3.234	0.24	H <sub>2</sub>	10.235	0.01	Fe II
3.296	1.05	HI 9-5 Pf $\delta$	10.509	82.2	S IV
			11.491	0.16	Ca V
3.498	0.14	H <sub>2</sub>	11.761	0.97	Cl IV
3.543	0.41	He II 13-9	12.28	1.52	H <sub>2</sub>
3.657	0.28	Al V	12.806	149	Ne II
3.690	0.16	Al VIII	13.095	33.3	Ar V
3.738	1.76	HI 8-5 Pf $\gamma$	13.515	5.73	Mg V
3.905	0.17	HI 15-6	14.314	634	Ne V
3.934	0.15	Si IX	14.358	1.6	Cl II
4.018	0.17	HI 14-6	14.388	27.0	Na VI
4.036	0.23	HeI	14.785	0.60	Fe VI
4.050	15.2	HI 5-4 Br $\alpha$	15.38	<1	K IV
4.085	0.28	Ca VII	15.547	377	Ne III
4.158	0.60	Ca V	17.025	1.39	H <sub>2</sub>
4.294	1.04	He I 5p-3s	17.936	0.30	Fe II
4.486	9.92	Mg IV	18.709	57.7	S III
4.529	86.5	Ar VI	20.365	<0.3	Cl IV
4.615	1.25	K III	20.812	0.50	Fe V
4.653	3.2	HI 7-5 Pf $\beta$	21.29	<0.3	Na IV
4.683	14.1	Na VII	21.808	2.99	Ar III
4.762	2.52	He II 8-7	22.93	<1.0	Fe III
5.128	0.66	HI 10-6	24.305	308	Ne V
5.445	<0.3	Fe VIII	25.878	322	O IV
5.500	40.8	Mg VII	25.981	2.6	Fe II
5.577	1.79	K VI	33.487	20.4	S III
5.606	51.0	Mg V	34.813	17.4	Si II
5.907	0.99	HI 9-6	35.966	21.0	Ne III
5.979	1.13	K IV			

were increased by 20%. The intensities so obtained are given in Table 1.

**Table 2.** NGC 6302, comparison of ISO with IRAS LRS and other observations. Intensities are in units of  $10^{-10}$  erg cm $^{-2}$  s $^{-1}$ 

Line	Ident.	ISO	IRAS	AH <sup>a</sup>	RHH <sup>b</sup>	DLW <sup>c</sup>
2.48	Si VII	0.23		0.43		
4.05	Br $\alpha$	0.126		0.169		
10.5	S IV	1.09	2.1			
12.8	Ne II	1.51	2.0			
14.3	Ne V	6.34	6.4			
15.5	Ne III	3.78	2.9			
18.7	S III	0.58	1.5:		0.69	
24.3	Ne V	3.08			3.23	
51.8	O III	1.65(LWS <sup>d</sup> )				0.73

<sup>a</sup> Ashley & Hyland (1988): diaphragm  $\sim 12''$

<sup>b</sup> Rowland et al. (1994): diaphragm  $\sim 28''$

<sup>c</sup> Dinerstein et al. (1985): diaphragm  $\sim 45''$

<sup>d</sup> Liu (1997)

As can be seen from Table 1, almost 100 lines have been detected with a range of about  $10^4$  in intensity. In addition, upper limits are given for 9 lines, which may be interesting for abundance determinations. Identifications are given in the table for most of the lines. Only 5 faint lines could not be identified. In addition to hydrogen and helium lines, 12 molecular hydrogen lines were seen. Further, 12 other elements were seen covering 40 ionization stages from neutral atoms to some with 300eV ionization potential. The resolution is sufficient so that there can be no doubt as to the identification of the lines. Only one case of important blending was found: the 8.988  $\mu$ m line contains a contributions of both Ar III and Mg VII.

Although the resolution is sufficient to measure the radial velocity, it cannot be done in this case. The reason is that line shifts are introduced by the position of the source in the aperture. A  $4''$  shift can introduce a line shift corresponding to 50 km s $^{-1}$ .

#### 4. Comparison with other infrared observations

In Table 2 we have listed the lines for which a comparison with other measurements is possible. In Column 4 of the table the IRAS low resolution measurements are listed. They differ slightly from what is reported in Pottasch et al. (1986) because the final reduction of the spectrum was used. Within the uncertainty of the measurements which we estimate to be 25% for ISO and somewhat more for the IRAS observations (especially for S III for which the IRAS uncertainty is large), there is agreement for all the lines except S IV at 10.544  $\mu$ m. This is remarkable in two ways, since the IRAS has a beam of at least 2 arc min, and thus has measured the entire nebula. Thus one might conclude that the ISO has also measured the entire nebula, at least in the Ne II, Ne III and Ne V lines, which is only marginally consistent with the discussion in the previous section. The large intensity of the S IV line as measured by IRAS is difficult to explain as due to the increased beam size, since in this case the increase in intensity should also be seen in the Ne II and Ne III lines.

Ashley & Hyland (1988) have measured the intensity of the Si VII and Brackett  $\alpha$  lines with an equivalent diaphragm of 12

**Table 3.** Hydrogen line intensities,  $10^{-12}$  erg cm $^{-2}$  s $^{-1}$ 

$\lambda$	Transition	Ident.	Obs.	Corr.	$T_e = 20\,000$ K
4.052	5-4	Br $\alpha$	12.6	13.5	(14.4)
2.626	6-4	Br $\beta$	5.9	6.7	8.65
7.457	6-5	Pf $\alpha$	5.5	5.6	4.37
4.653	7-5	Pf $\beta$	3.2	3.4	2.92
3.741	8-5	Pf $\gamma$	1.8	1.9	1.97
3.297	9-5	Pf $\delta$	1.1	1.2	1.38
3.039	10-5		0.66	0.73	1.01
2.873	11-5		0.55	0.63	0.76
2.758	12-5		0.43	0.49	0.58
2.564	15-5		0.31	0.36	0.29
4861Å	4-2	H $\beta$			234

arc sec. Their results, shown in Column 5, are similar to the ISO results. Rowland et al. (1994) have measured the S III and Ne V lines (Column 6) with a large diaphragm, about 28 arc sec diameter, and their intensities are almost the same as the ISO result. This would lead to the conclusion that ISO is measuring most of the light in these lines.

Finally Dinerstein et al. (1985) have measured the O III line at 51.8  $\mu$ m with the KAO in 1982 using a diaphragm of about 50 arc sec. Their intensity is about a factor of 2.5 lower than the ISO LWS measurement which has a large enough diaphragm to measure the entire nebula. Either one of these measurements are wrong or the nebula has changed considerably in 14 years.

#### 5. Comparison of hydrogen and ionized helium with theory

This comparison is made for several reasons. Firstly, it is interesting to see how well the line ratios agree with the theory. Secondly the ratios can then be extended to lines in the visual and ultraviolet spectrum (e.g. H $\beta$ ,  $\lambda$ 4686 and  $\lambda$ 1640) to predict the intensity of these lines in an aperture of the ISO size. This will make it possible to use the visual and ultraviolet spectrum in conjunction with the ISO spectrum.

##### 5.1. The hydrogen line spectra

The hydrogen line intensities measured in the Brackett and Pfund series are shown in Table 3. Lines due to two higher series have also been measured. A small correction for extinction must be made. This was done using  $E(B - V) = 0.88$  (see Oliva et al. 1996). The results are given in Column 5 of Table 2. For comparison the predicted recombination line spectrum is shown in the last column, for an electron temperature of 20 000 K (Hummer & Storey 1987), normalized to the Brackett  $\alpha$  line. The agreement is seen to be quite good, usually within a 30% uncertainty. The same theoretical spectrum predicts an H $\beta$  intensity of  $2.34 \times 10^{-10}$  erg cm $^{-2}$  s $^{-1}$ . The observed 6 cm. radio continuum flux of 3.0 Jy (Rodriguez et al. 1985) would predict an H $\beta$  intensity about twice as high:  $5.95 \times 10^{-10}$  erg cm $^{-2}$  s $^{-1}$ . This leads to the conclusion that the ISO diaphragm is only seeing one half of the hydrogen present. But such a conclusion is only correct when the extinction is uniform over the entire

**Table 4.** Helium line intensities

$\lambda$ $\mu\text{m}$	Transition	Obs.	Corr.	$T_e = 20\,000\text{ K}$ ( $10^{-12}\text{ erg cm}^{-2}\text{ s}^{-1}$ )
3.092	7-6	3.25	3.63	4.64
4.764	8-7	2.52	2.61	2.06
2.826	9-7	1.22	1.40	1.47
6.948	9-8	1.40	1.40	1.00
3.544	13-9	0.41	0.44	0.25
3.145	14-9	0.10	0.11	0.20
4686 Å	4-3			140
1640 Å	3-2			1040
3204 Å	5-3			62.4
2734 Å	6-3			33.8
2512 Å	7-3			20.3

nebula. This is far from being the case, as can be seen from the fact that the radio image has a strong emission peak at the centre (see Fig. 1) while the optical image shows a lack of emission, a dark lane, running through the centre. The extinction is thus much higher in the center, and the use of an average value of extinction could lead to an incorrect conclusion. Thus the ISO diaphragm could contain substantially more than half of the hydrogen present. It is possible to use maps of the Balmer decrement to obtain the extinction as a function of position in the nebula, and then form a weighted average over the ISO diaphragm. But this is an uncertain procedure and we have chosen not to use it. Instead we have chosen to relate the hydrogen and helium lines in the various spectral regions to their theoretical values, thus circumventing the extinction problem.

There is other evidence that the hydrogen emission is more extended than the ISO diaphragm. Danziger et al. (1973) measure an  $H\beta$  intensity, before correction for extinction, of  $1.70 \times 10^{-11}\text{ erg cm}^{-2}\text{ s}^{-1}$  with an aperture of  $17'' \times 34''$ . Copetti (1990), using  $100''$  diaphragm measure an  $H\beta$  intensity of  $2.95 \times 10^{-11}\text{ erg cm}^{-2}\text{ s}^{-1}$ , almost twice as high.

The extent derived from the hydrogen lines is in contrast with the compactness observed in the dust continuum (see Sect. 2.1). Physically this is possible if the dust density falls off faster than the gas density. But then the fact that the neon lines do not appear to extend beyond the SWS aperture must still be explained. One possible explanation is that the chemical composition of the outer nebular region is significantly lower than the inner region. This must be investigated further.

### 5.2. The ionized helium spectrum

The 6 observed lines of the He II spectrum are listed in Table 4. The 4 strongest lines show good agreement with the theoretical spectrum of  $T_e = 20\,000\text{ K}$  (Hummer & Storey 1987), which is shown in the last column of the table. This has been normalized to best fit these 4 lines. The theoretical value of the He II  $\lambda$  4686 line which corresponds to this normalization is also shown in this table. The ratio of  $\lambda$  4686/ $H\beta$  implied by the infrared lines is 0.60 (Tables 3 and 4). This is in reasonable agreement with what is observed after correction for reddening: 0.65 (Danziger

et al. 1973) and 0.73 (Aller et al. 1981). Thus if the hydrogen emission is more extended than the ISO diaphragm (conclusion previous section), the He II emission is also more extended.

The theoretical spectra in both Tables 3 and 4 have been given for  $T_e = 20\,000\text{ K}$ , which is close to the observed O III temperature of  $17\,000\text{ K}$ . The spectrum is not very sensitive to the temperature, and the conclusions do not change when the theoretical spectra for  $T_e = 15\,000\text{ K}$  is used. On the other hand, the observed line ratios cannot be used to fix the temperature.

## 6. The IUE spectrum

Of the 29 spectra in the IUE archive, not all are useable, mainly because they were underexposed. The remaining spectra have been taken in essentially 4 regions of the nebula. We will concern ourselves here with those spectra which were taken near the centre of the nebula, essentially the same position as the ISO observations. These are for the low resolution: SWP 05211, 10381, 30987, LWR 04506, 09063, 09064, LWP 10778. For the high resolution 2 spectra are available: SWP 08971 and 10391. Several of these spectra have been discussed earlier; Aller et al. (1981) and Barral et al. (1982). Two of the spectra were taken later (1987) and have not been discussed earlier.

The newly reduced spectra have been averaged. In this way it has been possible to reduce the noise compared to the earlier observations, making it possible to see weaker lines. The resultant measurements from the low resolution spectra are listed in Table 5. The wavelengths, in the first column, have an uncertainty of several angstroms. Because the total width of the low resolution spectral lines is 6 to 12 Å, close doublets (or multiplets) are summed and given as a single line. This is true of the first 4 lines in the table, and many other lines as well. The measured intensity refers to the average of the individual spectra, and probably has an uncertainty less than 20% for the strong lines. The weaker lines may have an uncertainty of 50%. The 3 lines marked with a colon (:) are barely visible and the intensities are uncertain by a factor 2. The lines for which no identification is given are all very weak.

These intensities may be compared to those given by Aller et al. (1981) and Barral et al. (1982). Since these authors used only one or two of the spectra, it is not surprising that our measurements usually lie between those given by them.<sup>1</sup> The principal difference between our measurements and theirs are the substantially increased number of lines reported here, which is the consequence of the increased signal to noise ratio of the combined spectra.

The last column of Table 5 gives the intensity of the lines after correction for (1) extinction, and (2) normalization. This is obtained in the following manner. It is assumed that the extinction  $E_{B-V}$  is known, as well as the extinction “law” as a function of wavelength. The value of the 4 He II lines is known from the ISO measurement (see Table 4), which also predicts

<sup>1</sup> Note that Aller et al. (1981) give a factor 10 too low intensity for O III 3133 and He II 3203 in Column 4 of their Table 2. Their further use of these intensities indicate that this was simply a typographical error.

**Table 5.** Ultraviolet (IUE) intensities, Measured Intensity in units of  $10^{13}$  erg cm $^{-2}$  s $^{-1}$ , Normalized Unreddened Intensity in units of  $0^{12[D]}$  erg cm $^{-2}$  s $^{-1}$ .

Wavel. Å	Ident.	Measured Intensity	Norm. Unreddened. Intens.
1239	N V	6.6	2260
1400	O IV	3.3	380
1485	N IV]	16.4	1450
1549	C IV	20.0	1515
1575	[Ne V]	1.1:	76
1600	Ne IV	1.9:	130
1610	?	1.0:	67
1640	He II	16.7	1070
1666	O III]	4.4	275
1750	N III	16.0	985
1806	?	1.3	86
1892	Si III]	0.9	76
1908	C III]	12.6	1070
2326	C II, O III, Fe III	0.8	60
2425	Ne IV	10.0	550
2470	O II	1.1	34
2512	He II	1.3	21
2636	Ar V	0.7	13
2676	?	0.3	5
2692	Ar V	0.3	5
2733	He II	2.6	35
2783	Mg V	3.3	43
2800	Mg II	0.8	10
2834	Fe IV, O III	2.2	23
2853	Ar IV	1.7	18
2869	Ar IV	1.1	12
2928	Mg V	1.3	13
2942	?	1.0	9
2974	Ne V	1.7	15
2998	?	0.5	4
3023	O III	1.4	14
3047	O III	3.7	34
3133	O III	21.4	171
3203	He II	9.0	65
3242	Na IV	2.7	14

what the strength of the unreddened ultraviolet lines will be in the ISO aperture. Thus with the extinction law of Seaton (1979) and a value  $E_{B-V} = 0.88$ , the normalized unreddened intensity given in Table 5 is obtained. Considering the uncertainties in the extinction law (part of the extinction is certainly local) it is not useful to try to do better than this. The good agreement of the 4 ultraviolet He II lines indicates that the method works to within 20% over most of the wavelength range. Only the 3 very short wavelength lines could have higher errors, but this is just the region where the extinction law is the most poorly known.

## 7. The visual spectrum

Many spectra have been taken in the “visual”. The principal difficulty is that the precise position is often not given, and the aperture is usually different, or not given. Thus if the spectrum

varies strongly with position, it is difficult to form a composite spectrum. Happily, the spectra prove to be relatively uniform.

The 6 most extensive spectral measurements in the visual are listed in Table 6. The positions and diaphragms used are as follows. Danziger et al. (1973) used a  $17'' \times 34''$  diaphragm centered at the brightest point. It was aligned east-west and thus included the entire “core” region measured by ISO and the IUE. In fact, as shown in Table 7, the Danziger et al. measurements represent about 60% of the total nebular emission (as represented by the measurements of Copetti (1990) which had a diaphragm which included the entire nebula). The measurements of Bohigas (1994) were made with a  $10'' \times 10''$  diaphragm, centered both at the “core” and at the brightest region. In Table 6, the measurements made at the “core” are given, but there is no difference between the spectra at the two positions to within the accuracy of the measurements. The spectra taken by Acker et al. (1989b) refer to a  $4'' \times 4''$  region, probably at a bright position. As can be seen from Table 7, only about 10% of the nebular radiation falls within this diaphragm. The spectrum reported by Oliva (1998, private communication, see also Reconditi & Oliva, 1993 and Oliva et al., 1996) was taken with a slit, whose width was 1.5 arcsec. The intensity extracted was averaged over the central 7 arcsec. Aller et al. (1981) measured with a slit in the “brightest region”, but further details are not given. In de Freitas Pacheco et al. (1991) a position is reported which is so far from the PN that it must be wrong. The actual position, as well as the diaphragm used, is thus unknown.

In spite of the variations in position measured and diaphragm size used, a surprisingly good agreement in the measured spectrum is seen in Table 6. This fact, coupled with the measurement by Bohigas that no substantial spectral differences between the “core” and the brightest region are found, provide the basis for giving an “average” visual spectrum. This average spectrum has been corrected for extinction and normalized in the same way as described in the previous section for the IUE spectrum. The corrected, normalized spectrum is given in the last column of Table 6.

## 8. Discussion and conclusion

Tables 1, 5 and 6 form an integrated spectrum of the central regions of NGC 6302, from  $\lambda = 1240$  Å through  $\lambda = 36$  μm. These intensities are normalized to the ISO aperture and corrected for extinction in a manner which gives much weight to the H and ionized He spectrum. They refer, as much as possible, to the same region of the nebula. In spite of the large and uncertain extinction to the nebula, the method used limits the errors, which are probably less than 50% in the extreme (except for very faint lines). This can be checked. There are at least 5 pairs of lines in different regions of the spectrum, which are emitted from the same level of the same ion. The intensity ratio of these is thus only determined by the atomic transition probability (Einstein A value). Since these values are accurately known, we can compare the predicted ratio with the observed ratio. This is shown in Table 8, where the different ions, upper levels and wavelengths of the lines involved, are given in the first 3 columns.

**Table 6.** Observed Visual Spectrum. The Normalized Unreddened Intensity is in units of  $10^{-12}$  erg cm $^{-2}$  s $^{-1}$ 

$\lambda$	Aller et al. (1981)	Danziger etal.(1973)	Freitas Pacheco etal. (1991)	Acker et al. (1989b)	Oliva (1998)	Bohigas (1994)	Norm. Unred. Intens.	
3204	He II	9.8					77	
3242	Na IV	0.72					5.5	
3346	Ne V	39.0					266	
3362	Na IV	0.33					2.2	
3426	Ne V	110					700	
3727	O II	30.5				28.9	146	
3869	Ne III	61.0					230	
4163	K V	0.25					1.0	
4340	H $\gamma$	32.4	34.7	45.6	33		11.5	
4363	O III	27.8	28.2		24		95	
4471	He I	4.5	4.9		4		15	
4686	He II	65	59	69	59	72	60	160
4725	Ne IV	3.4				3.9		9.4
4740	Ar IV	19.5			22	20		52
4861	H $\beta$	100	100	100	100	100	100	240
5007	O III		1476	1727	1354	1380	1670	3110
5192	Ar III					0.63		1.2
5755	N II			44	34	27		44
5875	He I			32.5	37	25	32	43
6312	S III			7.3	11	11.8		11.5
6565	H $\alpha$			1114	704	735	933	720
6584	N II			1798	1758	1051	1481	1230
6724	S II			140	163		131	140
7005	Ar V			34	34	36		27.6
7065	He I				31	27		22.6
7136	Ar III			111	92	78.7		62
7237	Ar IV				3	4.0		2.7
7320	O II			70		30.9		22.5
7330	O II			70		27.2		19.8
9533	S III					426		172
9918	S VIII					10.3		3.7

**Table 7.** Measured H $\beta$  and O III line intensities

Observer	Diaphragm	F(H $\beta$ )	F(O III)
(1)	100''	$2.95 \times 10^{-11}$	$3.89 \times 10^{-10}$
(2)	17'' $\times$ 34''	$1.70 \times 10^{-11}$	$2.51 \times 10^{-10}$
(3)	4'' $\times$ 4''	$2.82 \times 10^{-12}$	$3.82 \times 10^{-11}$

(1) Copetti (1990), (2) Danziger et al. (1973)

(3) Acker et al. (1989a)

The predicted ratio's, in Column 4, and the observed ratio's, in Column 5, are seen to be in good agreement. Even for the Ne IV and Ne V lines, where the intensities are quite uncertain, the agreement is acceptable.

We thus conclude that an acceptable spectrum has been obtained over the entire wavelength region, and referring, as well as the present observations allow, to the same aperture. It is this spectrum which will be used to derive the element abundances in NGC 6302.

*Acknowledgements.* We thank Dr. P. Perinotto for his careful reading of the manuscript and his suggestions for clarifying the text.

**Table 8.** Predicted and observed line ratio's

Ion	Upper Level	Line Wavel. (Å)	Predicted Ratio	Observed Ratio
O II	$p^3(^2P_{1/2} + ^2P_{3/2})$	2471/(7320 + 7330)	0.75	0.83
Ar IV	$p^3 ^2P_{1/2}$	2869/7264	3.62	3.53
Ar IV	$p^3 ^2P_{3/2}$	2854/7237	8.87	6.7
Ne IV	$p^3(^2P_{3/2} + ^2P_{1/2})$	1601/4725	6.4	13:
Mg V	$p^4 ^1D_2$	2783/2928	3.59	3.46
Ne V	$p^2 ^1S_0$	1575/2974	2.8	5:

## References

- Acker A., Stenholm B., Tylenda R., 1989a, A&AS 77, 487  
Acker A., Jasniewicz G., Koppen J., Stenholm B., 1989b, A&AS 80, 201  
Aller L.H., Ross J.E., O'Mara B.J., Keyes C.D., 1981, MNRAS 197, 95  
Ashley M.C.B., Hyland A.R., 1988, ApJ 331, 532  
Barral J.F., Canto J., Meaburn J., Walsh J.R., 1982, MNRAS 199, 817  
Bohigas J., 1994, A&A 288, 617  
Copetti M.V.F., 1990, PASP 102, 77  
Danziger I.J., Groegel J.A., Persson S.E., 1973, ApJ 184, L29  
Dinerstein H.L., Lester D.F., Werner M., 1985, ApJ 291, 561

- Hummer D.G., Storey P.J., 1987, MNRAS 224, 801
- de Freitas Pacheco J.A., Maciel W.J., Costa R.D.D., Barbuy B., 1991, A&A 250, 159
- Liu X.-W., 1997, ESA Sp-419, p. 87
- Oliva E., Pasquali A., Reconditi M., 1996, A&A 305, L21
- Pottasch S.R., Preite-Martinez A., Olnon F.M., et al., 1986, A&A 161 363
- Pottasch S.R., Beintema D., Dominguez-Rodriguez F.J., et al., 1996, A&A 315, L261
- Rodriguez L.F., Garcia-Barreto J.A., Canto J., et al., 1985, MNRAS 215, 353
- Reconditi M., Oliva E., 1993, A&A 274, 662
- Rowland N., Houck J.R., Herter T., 1994, ApJ 427, 867
- Seaton M.J., 1979, MNRAS 187, 785